

OPEN

CgSTE11 mediates cross tolerance to multiple environmental stressors in *Candida glabrata*

Mian Huang¹, Jibrán Khan², Manpreet Kaur³, Julian Daniel Torres Vanega^{4,5}, Orlando Andres Aguilar Patiño^{4,5}, Anand K. Ramasubramanian³ & Katy C. Kao^{3*}

Candida glabrata is a human commensal and an opportunistic human fungal pathogen. It is more closely related to the model yeast *Saccharomyces cerevisiae* than other *Candida* spp. Compared with *S. cerevisiae*, *C. glabrata* exhibits higher innate tolerance to various environmental stressors, including hyperthermal stress. Here we investigate the molecular mechanisms of *C. glabrata* adaptation to heat stress via adaptive laboratory evolution. We show that all parallel evolved populations readily adapt to hyperthermal challenge (from 47 °C to 50 °C) and exhibit convergence in evolved phenotypes with extensive cross-tolerance to various other environmental stressors such as oxidants, acids, and alcohols. Genome resequencing identified fixation of mutations in *CgSTE11* in all parallel evolved populations. The *CgSTE11* homolog in *S. cerevisiae* plays crucial roles in various mitogen-activated protein kinase (MAPK) signaling pathways, but its role is less understood in *C. glabrata*. Subsequent verification confirmed that *CgSTE11* is important in hyperthermal tolerance and the observed extensive cross-tolerance to other environmental stressors. These results support the hypothesis that *CgSTE11* mediates cross-talks between MAPK signaling pathways in *C. glabrata* in response to environmental challenges.

The ability to adapt to changing environments is essential for microbial survival. Temperature is an environmental variable that has profound impacts on the physiology of living organisms. If the temperature falls outside of the range an organism could tolerate, depending on the duration of exposure, damage to cellular components will ensue, eventually leading to cell death^{1,2}. In yeast, response to heat stress is most well studied in *S. cerevisiae*, in which the mitogen-activated protein kinase (MAPK) signaling pathways play critical roles³. There are currently 5 known MAPK signaling pathways in *S. cerevisiae*. In response to elevated temperatures, the cell wall integrity (CWI) and high-osmolarity glycerol (HOG) pathways^{4–6} are activated. The HOG pathway involves two independent branches, the Sho1 branch that involves osmosensors Hrk1 and Msb2⁷ and Sho1⁸, and the Sln1 branch with Sln1 as the osmosensor⁹. Heat stress activates the CWI pathway by two transmembrane sensors, Slg1¹⁰ and Mid2¹¹; deletion of components in this signaling cascade have been shown to result in slow growth at 30 °C and cell lysis at 37 °C^{5,12}. In addition, heat stress also activates Hog1, the MAPK of HOG pathway, via the Sho1 branch, but not the Sln1 branch⁶. The heat stress-activated Hog1 contributes to the rapid cell recovery from the challenge; interestingly, it is not localized in the nucleus after activation in response to heat, suggesting that the phenotypic effects are not due to its direct downstream transcriptional regulations⁶. The cross-talk between the HOG and CWI signaling pathways upon heat stress was recently elucidated to be mediated by Nst1 in *S. cerevisiae*¹³. In addition to signaling pathways, the heat stress response (HSR) in *S. cerevisiae* involves several transcription factors, including Hsf1, Msn2, and Msn4, and their downstream targets^{14–16}. Temperature sensing mechanisms have also been proposed, such as the membrane fluidity change, unfolded protein responses, and RNA thermometer (reviewed in¹⁷).

C. glabrata is an opportunistic human fungal pathogen and is more closely related to *S. cerevisiae* than other *Candida* spp. It exhibits a higher inherent tolerance to various environmental stressors such as heat, organic

¹Artie McFerrin Department of Chemical Engineering, Texas A&M University, College Station, Texas, 77843, United States of America. ²Department of Biology, Texas A&M University, College Station, Texas, 77843, United States of America. ³Department of Chemical and Materials Engineering, San José State University, San José, CA, 95192, United States of America. ⁴Department of Chemical Engineering, Industrial University of Santander, Bucaramanga, Colombia. ⁵These authors contributed equally: Julian Daniel Torres Vanega and Orlando Andres Aguilar Patiño. *email: kao.katy@gmail.com

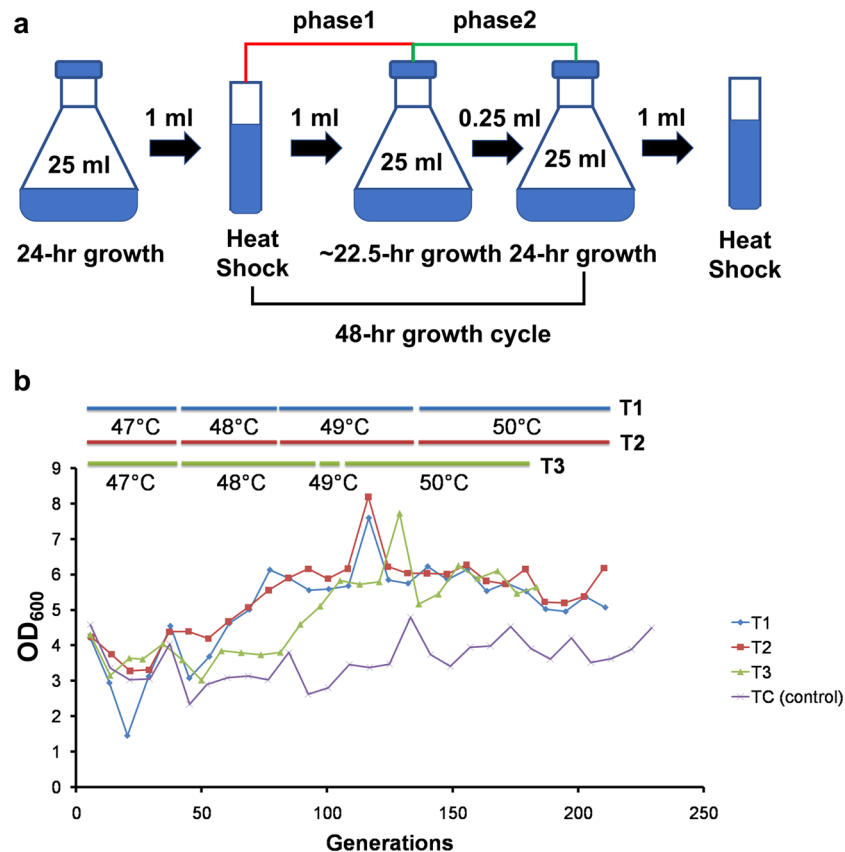


Figure 1. Adaptive laboratory evolution of *C. glabrata* to hyperthermal challenge. **(a)** The two-phase periodic heat challenge strategy used for adaptive evolution of *C. glabrata*. **(b)** Changes in the population cell density (OD_{600}) during the adaptive evolution of *C. glabrata*. The temperature used for periodic hyperthermal challenge are shown as colored bars (blue for T1, red for T2, and green for T3) above the graph. The control population TC was transferred in the absence of periodic hyperthermal challenge.

acids, low pH, and oxidant, compared with *S. cerevisiae*^{18,19}. Homologs of many central components of the MAPK pathways (e.g. HOG and CWI pathway) and major regulators of general stress response (e.g. Msn2, and Msn4) in *S. cerevisiae* are found in *C. glabrata* based on their amino acid identities or through the few existing functional characterizations^{18,20}. Prior study found growth to be unaffected by deletion of *SHO1*, the gene encoding the osmosensor and scaffolding protein within the Sho1 branch of HOG pathway⁸, at 37°C, but is significantly inhibited at 42°C, demonstrating that the Sho1 branch of HOG signaling in *C. glabrata* influences cellular tolerance to high temperature²¹. The *C. glabrata* Msn2 and Msn4 orthologues have also been found to be involved in the regulation of gene expression in response to multiple stresses, including heat, osmotic, oxidative, and glucose starvation²⁰. While the few existing studies have identified several cellular components involved in stress tolerance in *C. glabrata* based on knowledge in *S. cerevisiae*, the regulatory and signaling pathways involved in response to environmental stressors, including heat, are still largely unknown in this important yeast.

In this work, we harnessed the power of adaptive laboratory evolution to uncover the molecular mechanisms of *C. glabrata* adaptation to heat stress using periodic hyperthermal challenge. The results showed that *C. glabrata* readily adapts to step-wise increases in heat challenge (from 47°C to 50°C). Interestingly, the hyperthermal tolerant mutants isolated from parallel populations exhibited convergence in evolved phenotypes with extensive cross-tolerance to other environmental stressors. Mutations in the MAPK kinase *CgSTE11* were found in all parallel populations, suggesting the importance of this gene in hyperthermal tolerance. Subsequent verification via site-directed mutagenesis confirmed that mutations in *CgSTE11* played a major role in the hyperthermal tolerance and the observed cross-tolerance to other environmental stressors, providing strong evidence that *CgSTE11* mediates cross-talks between MAPK signaling pathways in *C. glabrata* in response to environmental stressors.

Results

Adaptive evolution of *C. glabrata* in periodic hyperthermal challenge. Three parallel populations (T1, T2, and T3) were evolved in YNB medium at elevated temperatures via serial batch transfers for more than 180 generations. Visualizing evolution in real-time (VERT)²² was used to track the population dynamics during evolution using two otherwise isogenic strains that are labeled with either yellow fluorescent protein (YFP) or green fluorescent protein (GFP). An adaptive evolutionary strategy using periodic challenge at high temperatures ($\geq 47^\circ\text{C}$) was employed (see Fig. 1a and Materials and Methods for details). A control population (TC) serially

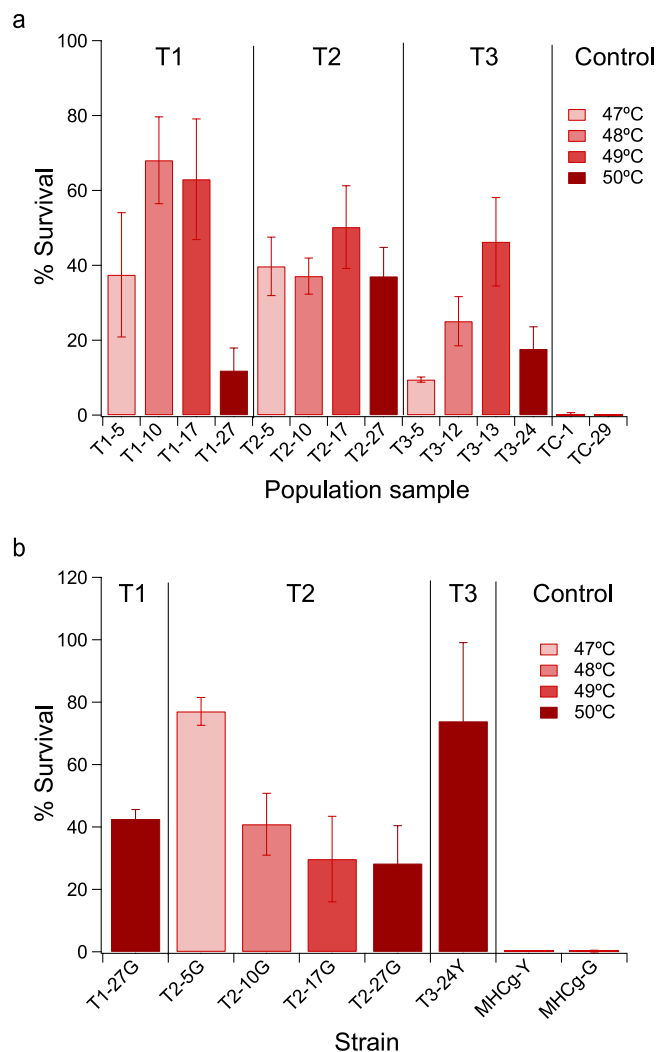


Figure 2. The survival rates of evolved populations (**a**) and isolated adaptive mutants (**b**) after 1-hr heat shock treatments at the specified temperatures. The data shown is the mean survival rates based on three biological replicates. The controls TC-1 (1st sample from the control population), TC-29 (last sample from the control population), and parental strains MHCg-Y and MHCg-G were challenged at 47 °C.

transferred at 30 °C without periodic hyperthermal challenge was included. Whenever a significant increase in cell growth (based on OD_{600} measurements at the end of Phase 1) was observed during the course of evolution (Fig. 1b), the viability of evolving population after heat exposure at various temperatures was measured and compared with the parental strains to determine whether the population exhibited improved hyperthermal tolerance (see Materials and Methods for details). If an improvement was observed, the selective pressure (temperature) was ramped up accordingly.

The evolutionary dynamics of all populations were estimated by quantifying the relative proportions of GFP- and YFP-colored subpopulations (Figs S1–S4). Any increase in the relative proportion of a colored-subpopulation is suggestive of the emergence and expansion of hyperthermal tolerant mutants within the population (an adaptive event). In populations T1 and T2, rapid sweeps by the GFP-colored subpopulation were observed early on during the evolution. Interestingly, there was a lack of significant increases in OD_{600} observed in T1 and T2 populations before generation ~37 even though expansion was observed in the GFP-subpopulations, suggesting that VERT is more sensitive in detecting adaptive events. However, due to the rapid sweep of one of the colored-subpopulations in 2 out of 3 parallel populations, use of VERT data to identify subsequent adaptive events in the population was not possible, thus increases in OD_{600} values were used instead. In population T3, the expansion and contractions of the GFP and YFP-colored subpopulations correlated fairly well with the OD_{600} data.

Phenotypic characterizations of adaptive mutants. At the end of the evolution experiment, the population samples prior to each ramp-up in selective pressure were revived from frozen stocks. The viability of each population after one-hour exposure to the temperature that the time-course sample was challenged with during evolution was quantified. All populations tested gained significantly improved tolerance to heat challenge (Fig. 2a). Population T2-27 (from population T2, sample 27) exhibited the highest thermotolerance with

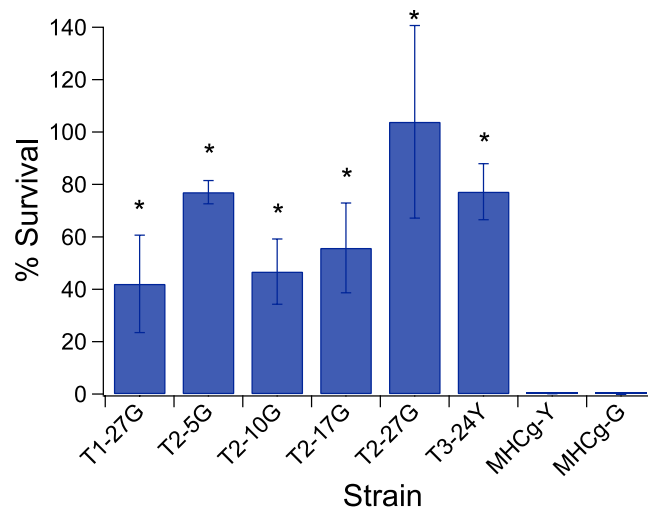


Figure 3. The survival rates of adaptive mutants and parental strains (MHCg-Y and MHCg-G) after 1-hr heat shock treatments at 47°C. The data shown is the mean survival rates from at least three biological replicates. Asterisks indicate that the survival rates of adaptive mutants are statistically different from the parental strain, MHCg-G or MHCg-Y (p-value < 0.05, unpaired student t test with unequal variance).

Strain ID	Oxidative Shock	Acid Shock		Solvent Shock			Osmotic Stress		Antibiotics	
	H ₂ O ₂ (100 mM)	HCl (pH~1)	Acetic acid (pH~3)	EtOH (16%, v/v)	1-butanol (4%, v/v)	Isobutanol (4%, v/v)	Glucose (30%, w/v)	Sorbitol (2 M)	AmB (0.25–32 µg/mL)	Flu (1–128 µg/mL)
T1-27G	++	>++++	++++	>+++	>+++	>++++	N	N	N	N
T2-5G	N	>++	+++	>+	N	>++++	N	N	N	N
T2-10G	++	>++	+++	>++	N	>++++	N	N	N	N
T2-17G	++	>++	+++	>+++	N	>++++	N	N	N	N
T2-27G	+	>+++	++++	>++++	N	>++++	N	N	N	N
T3-24Y	+	>+++	+++	>+++	>++	>++++	N	N	N	N

Table 1. Summary of cross-tolerance of isolated mutants. Note: AmB, amphotericin B; Flu, fluconazole; N, not more resistant than parental strains. The number of ‘+’ indicates the level of tolerance compared to the parental strain. Each ‘+’ represents ~10X increase in survival after the stress challenge.

an average viability of ~37% after heat shock at 50°C for 1 hour. In contrast, the average viability of the parental strains, MHCg-Y and MHCg-G, were ~0.35% after challenged at a much lower temperature (47°C) for 1 hour. Population T2 was chosen for more detailed time course characterizations.

Time course samples from population T2 and the end-point samples from T1 and T3 were selected for further phenotypic characterizations. Adaptive mutants T2-5G, T2-10G, T2-17G, and T2-27G were isolated from time points immediately prior to each ramp-up in selective pressure, from populations T2-5, T2-10, T2-17, and T2-27, respectively (Fig. S3). Adaptive mutants T1-27G and T3-24Y were isolated from the last time point samples of populations T1 and T3, respectively. Each adaptive mutant was analyzed for tolerance (survival) to 1-hour heat shock at the temperature at which they were challenged during the evolution. We observed significant increases in the viability after the heat challenge for all adaptive mutants tested when compared to the parental strains, MHCg-Y and MHCg-G (Fig. 2b). Among all the mutants tested, strain T3-24Y exhibited the highest viability after heat shock at 50°C, with an average survival rate of ~74%. The controls (MHCg-Y and MHCg-G) in this experiment exhibited survival rates of ~0.2% after heat challenge at 47°C for 1 hour. In addition, we also measured the viability of all the mutants after a 1 hour challenged at 47°C; the data showed that all of the mutants exhibited much higher survival rates compared to the parental strains (Fig. 3).

Cases of cross-tolerance to additional stressors were observed in prior adaptive laboratory evolution studies in other species (e.g. *Escherichia coli*, *Salmonella typhimurium*, and *Corynebacterium glutamicum*)^{23–25}. For example, positive and negative cross-stress protection were observed in laboratory evolved *E. coli*²⁴; and *Corynebacterium glutamicum* evolved under thermal stress also exhibited cross-tolerance to isobutanol²⁵. Thus, we hypothesized that a genotype optimized for one phenotype (mutant evolved for tolerance to one stressor) may exhibit cross-benefit to other compatible phenotypes (cross-tolerance to other stressors). The evolved heat tolerant mutants were tested against a wide range of stressors, including oxidative stress (H₂O₂), acids (HCl and acetic acid), osmotic (glucose and sorbitol), antifungal drugs (amphotericin B and fluconazole), and solvents (ethanol, 1-butanol, iso-butanol), to assess their level of cross-tolerance to other stressors. Results are shown in Table 1 and Fig. 4. Compared to the parental strains, the evolved mutants exhibited significantly improved tolerance to many

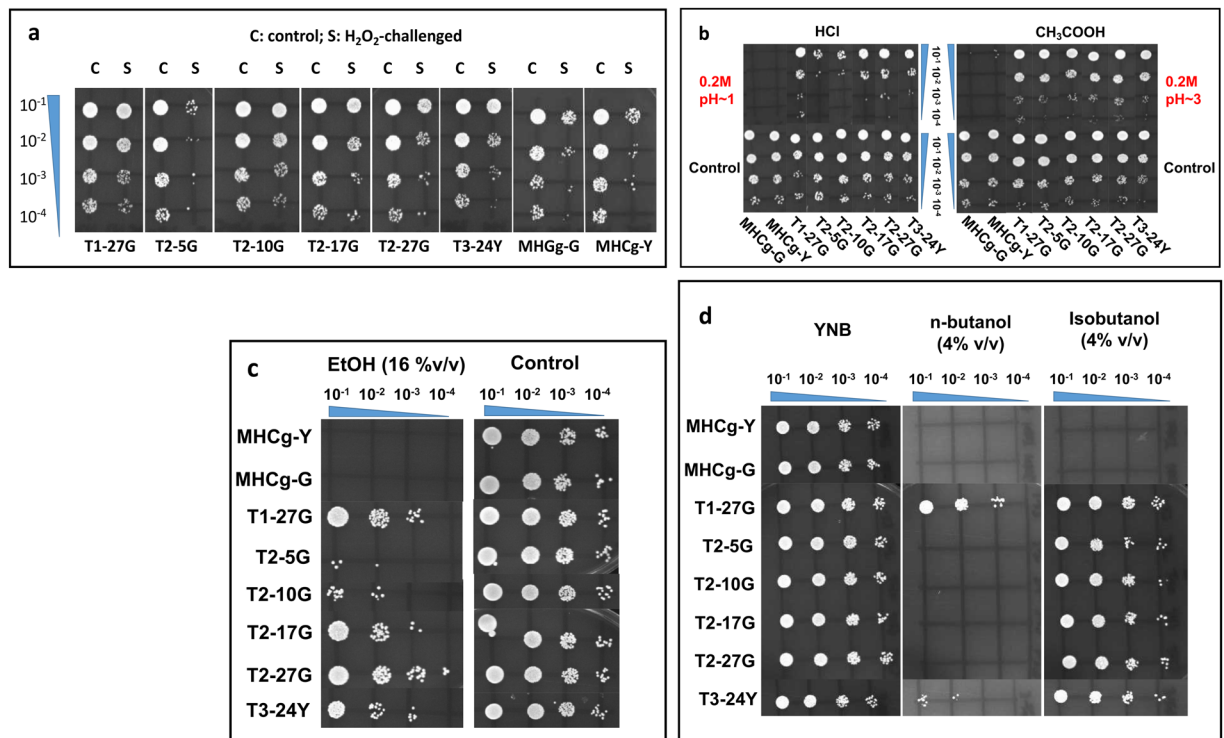


Figure 4. Cross-tolerance of isolated adaptive mutants and parental strains (MHCg-Y and MHCg-G) to H₂O₂ (a), HCl and acetic acid (b), ethanol (c), n-butanol and isobutanol (d). Each strain was subjected to 1-hour exposure to specified stressor, serial diluted, and plated on YNB medium supplemented with 2% dextrose at 30 °C for two days.

of these stressors. For some stressors tested (H₂O₂ and HCl), the results showed a gradual increase in the level of cross-tolerance to these stressors over time during the adaptive evolution to hyperthermal challenge in population T2. These results suggest that adaptation to thermal stress in *C. glabrata* may share similar mechanisms with adaptation to other stressors, possibly through common key components in stress sensing, signal transduction, and stress response.

The heat shock proteins (HSP) play crucial roles for cell survival in the presence of environmental stressors including heat. Thus, the adaptive mutants were heat challenged at 41 °C in the presence of the HSP90 inhibitor radicicol to determine if HSP90 is essential for the improved hyperthermal tolerance observed. Presence of radicicol resulted in no growth inhibition in any strains tested at normal growth temperature (30 °C), but completely inhibited the growth of all strains at 41 °C (Fig. 5), demonstrating that HSP90 is required for thermo-tolerance in *C. glabrata* and that the improved adaptation to hyperthermal stress in the adaptive mutants is HSP90-dependent.

Whole genome resequencing to identify potential beneficial mutations. All six isolated adaptive mutants and the parental strains MHCg-G and MHCg-Y were resequenced; and a total of 20 *de novo* mutations were identified from these adaptive mutants (Table S2). Among these mutations, 17 are in coding sequences and 2 are within 1 kbp of at least one coding sequence. Four mutations were identified in more than one adaptive mutant, three of which are present in two pseudogenes (CAGL0F00110g and CAGL0B05093g). One mutation in gene CAGL0B02739g (C766A) is present in all four adaptive mutants isolated from population T2. CAGL0B02739g encodes the homolog to the *S. cerevisiae* mitogen activated protein kinase kinase (MAPKKK/MEKK) Ste11p; CgSte11 is reported to function in hypertonic stress response, filamentous growth, and virulence in *C. glabrata*²⁶. Interestingly, mutations in CgSTE11 were also identified in the two adaptive mutants sequenced from population T1 (C1661T) and T3 (C766T); the mutation in CgSte11 in strain T3-24Y from population T3 (C766T, Pro256Ser) occurred at the same nucleotide position as that identified in mutants from population T2 (C766A, Pro256Thr), but with a different amino acid change. We also performed population-level sequencing to identify all mutations present at a minimum of 10% frequency in the population over the course of the evolution (raw sequencing data in SRA with the accession number of SRP112804). The time-course population-level sequencing results from T1, T2, and T3 revealed that the frequency of CgSTE11 mutations increased rapidly over time and fixed in all populations at the end of the evolution experiment, strongly suggesting that CgSte11 plays an important role in the adaptation of *C. glabrata* to heat stress (Fig. S5).

Gene Ontology (GO) analysis was performed using the ‘GO term Finder’ from the Candida Genome Database (<http://www.candidagenome.org/>) to identify any enriched biological processes or molecular functions among the genes with identified mutations in the coding regions or in potential regulatory regions in the mutants. The results revealed that genes functioning in the osmosensory signaling pathway (CAGL0H06567g,

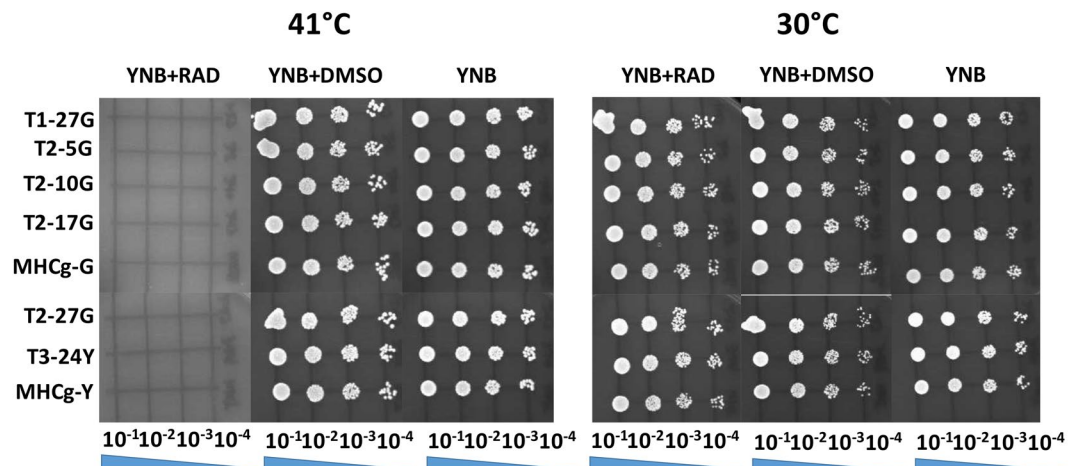


Figure 5. The effects of radicicol (RAD) on the thermotolerance of adaptive mutants and parental strains (MHCg-Y and MHCg-G). The cells were grown on YNB plates supplemented with 2% dextrose in the presence or absence of 5 μ M of RAD at both 30 $^{\circ}$ C and 41 $^{\circ}$ C.

CAGL0B02739g [*CgSTE11*], and CAGL0M11748g) are significantly enriched with a p-value of \sim 0.0028, which suggests the involvement of the components of the osmosensory signaling pathway in *C. glabrata* adaptation to heat stress. Among these genes, *CgSte11* has been shown to play a key role in the osmotic stress response in *C. glabrata*²⁶. Since the majority of the identified mutations are in genes that have not been characterized in *C. glabrata*, we performed our analysis based on the functions of their *S. cerevisiae* orthologs (from Saccharomyces Genome Database and Candida Genome Database) to search for mutated genes that potentially contributed to the improved environmental stress tolerance in *C. glabrata*. In total, we found 9 candidate genes whose orthologs are known to impact *S. cerevisiae* tolerance to at least one of the stressors tested (Table S3). Surprisingly, 5 of the 9 genes (CAGL0C05599g, CAGL0D06732g, CAGL0F03311g, CAGL0G08602g, and CAGL0H06281g) contain likely inactivating mutations (either nonsense or frame shift mutations). Null mutations in four of these genes are known to impair tolerance to some environmental stressors (e.g. ethanol, H₂O₂, HCl) in *S. cerevisiae*. Assuming the functions are conserved between the *C. glabrata* genes and their *S. cerevisiae* orthologs, these mutant alleles (except for CAGL0C05599g) may potentially decrease stress tolerance in *C. glabrata*; surprisingly, the adaptive mutants harboring these mutations exhibit increased tolerance to many of the same stressors. In contrast, CAGL0C05599g is predicted to be an ortholog to the *S. cerevisiae* *LRG1* gene, which has been reported to increase thermal and acetic acid tolerance when nullified^{27,28}. Thus, the nonsense mutation in CAGL0C05599g found in mutant T2-27G may be responsible for the improved tolerance to thermal and acetic acid stress in this mutant. In addition, mutations in 2 of the 9 genes (CAGL0M05709g and CAGL0M11748g) are missense mutations. The *S. cerevisiae* ortholog of CAGL0M05709g is *SGF73*, which has been reported to play a role in the resistance to H₂O₂ and ethanol^{29,30}. *HOG1* is the *S. cerevisiae* ortholog of CAGL0M11748g, and is known to impact the resistance of yeast to boric acid and H₂O₂^{29,31}.

Phenotypic effects of reconstructed *CgSTE11* mutants on general stress tolerance. The fixation of mutations in *CgSTE11* (CAGL0B02739g) in all 3 parallel populations and the enriched osmosensory signaling pathway, which *Ste11* in *S. cerevisiae* is a component of, from the GO analysis led us to speculate that the identified mutations in this gene are causative for the enhanced heat tolerance observed in the evolved mutants. Currently, genetic engineering tools are limited in *C. glabrata* compared with *S. cerevisiae*³². Thus, variants of the *CgSTE11* alleles were reconstructed in a wild-type background using a strategy based on the MoClo-derived assembly developed for *S. cerevisiae* (see Materials and Methods for details)^{33,34}. Specifically, *CgSTE11* C1661T (identified in the T1 population), *CgSTE11* C766A (identified in the T2 population), and *CgSTE11* C766T (identified in the T3 population) alleles were reconstructed in the parental background (ATCC 2001) to generate strains sMH081, sMH082, and sMH083, respectively. After looping out the SAT1 cassette, a scar of \sim 109 bp remained between the coding sequence of *CgSTE11* and the 3' UTR, which can potentially impact the expression of the gene³⁵. Thus, a control strain sMH80 was generated via the same procedure to reintroduce the wild-type allele into ATCC 2001, to assess any phenotypic impacts due to the presence of the FRT scar. These strains (sMH080, sMH081, sMH082, and sMH083) along with ATCC 2001 were subjected to short-term challenge to environmental stressors, and the results are shown in Fig. 6. No significant differences in the tolerance to any stressors were observed between ATCC 2001 and control strain sMH080, suggesting that the FRT scar did not significantly impact the expression of the gene. All 3 *CgSTE11* variants acquired increased tolerance to several stressors tested, including heat, hydrogen peroxide, ethanol, acetic acid, etc., as compared to both wild-type controls. The results demonstrate that mutations in *CgSTE11* contributed to the enhanced tolerance to various environmental stressors observed in the adaptive mutants. Tolerance assay using a *ste11* deletion strain showed that *ste11* Δ does not enhance hyperthermal tolerance in *C. glabrata* (see Supplementary Fig. S6), suggesting that the *CgSTE11* variants selected for are not inactivating mutations.

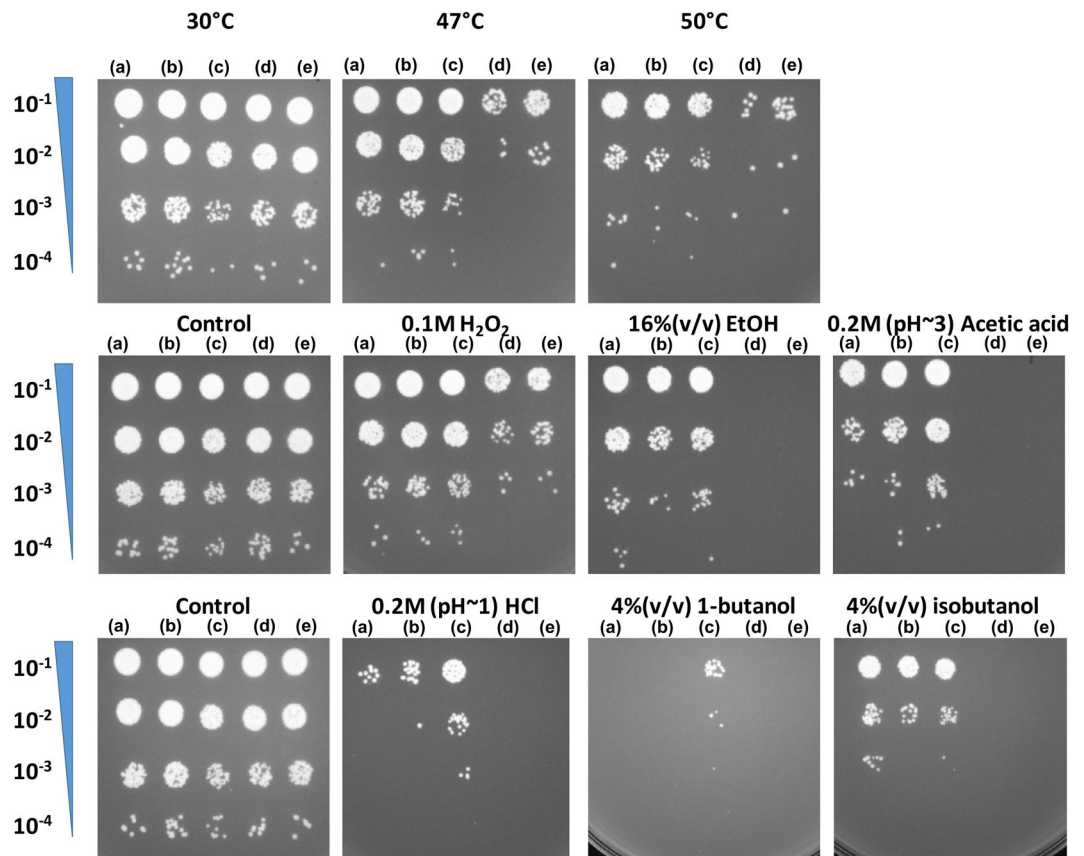


Figure 6. The stress tolerance for reconstructed *CgSTE11* mutants (sMH083 (a), sMH082 (b), sMH081 (c)) and the two controls, sMH080 (reconstructed wild-type; (d)) and ATCC 2001 (e) using 1-hr shock assays.

Phenotypic effects of reconstructed *CgSTE11* mutants on biofilm formation. In addition to high osmotic stress and cell wall stress response, MAPK signaling pathways have been shown to participate in adhesion^{36,37} and biofilm formation^{38,39} in *S. cerevisiae* and *C. albicans*. Expression of *ScSTE11* is downregulated in biofilm versus free planktonic cells³⁸. In *C. albicans*, a *CaSTE11* mutant exhibited stronger biofilm formation compared with the wild-type³⁹; interestingly, insertion mutants in *CaSTE11* showed significantly reduced adhesion compared with wild-type³⁷. The impacts of two of the adaptive mutations in *CgSTE11* (strains sMH081 and sMH082) on biofilm formation was assessed using biofilm quantification assay with crystal violet staining. Control strains ATCC 2001 and sMH080 along with *ste11Δ* were also analyzed. Results show no significant difference between biofilm formation in ATCC 2001 and sMH080 as expected (Fig. 7). The *ste11Δ* strain exhibited higher biofilm formation, whereas strains sMH081 and sMH082 showed slight decrease in biofilm formation compared with the wild-type controls. The results showed that similar to *S. cerevisiae* and *C. albicans*, Ste11 also plays a role in biofilm formation in *C. glabrata*.

Discussion

In this work, we identified and confirmed that mutations in *CgSTE11* found in hyperthermal evolved mutants contribute to enhanced tolerance to a wide range of environmental stressors and that the MAPK kinase kinase likely plays a key role in cellular response to environmental stressors in *C. glabrata*. *CgSte11* is assumed to be a key component in the Sho1 branch of HOG signaling pathway based on its ability to partially complement the loss of Ste11 in *S. cerevisiae*²⁶. In addition to osmotic stress, the HOG signaling pathway in *S. cerevisiae* is also activated in response to oxidative stress^{40,41}, and exposure to acetic acid (through the Sln branch)⁴². It has been shown that the Sho1 branch of HOG signaling in *C. glabrata* influences cellular tolerance to heat and weak organic acids²¹. Thus, it is likely that *CgSte11* functions in the modulation of heat and weak acid tolerance. In agreement with this theory, our experimental results showed that the heat tolerance conferring mutations in *CgSTE11* also significantly improved the tolerance of *C. glabrata* to acetic acid, suggesting that the mutated *CgSTE11* may improve stress tolerance, at least to heat and weak acid, by increasing the activity of HOG signaling in *C. glabrata*. It is important to note that strain ATCC 2001 used in this work has a truncated *CgSsk2* allele, resulting in an inactive Sln1 branch of the HOG1 signaling pathway²¹. Thus, it is possible that the impact on weak acid tolerance conferred by the *CgSte11* variants may be obviated in a strain with an active Sln1 branch. Further investigation in a different background will verify whether a bypass through this other HOG1 branch will impact the effects of the *CgSte11* variants on organic acid tolerance observed in ATCC 2001. Studies have shown that *CgSte11* is required for tolerance to hyperosmotic stress, nitrogen starvation induced filamentation, and virulence in *C. glabrata*²⁶.

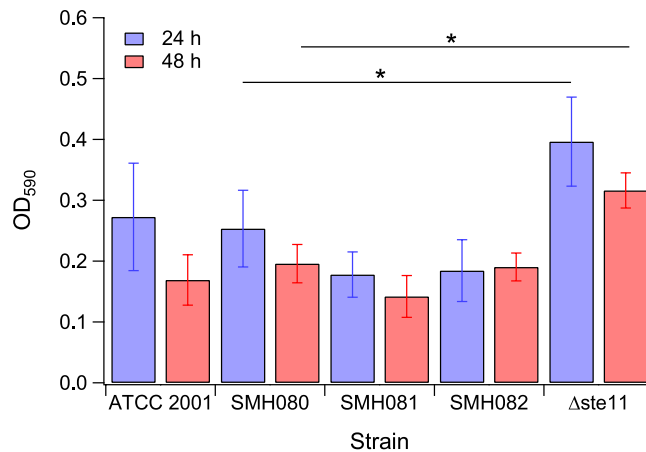


Figure 7. Biofilm formation of *CgSTE11* wild-type (ATCC 2001 and sMH080), reconstructed mutants (sMH081 and sMH082), and *ste11Δ* strains. Blue bars: 24 hour biofilms. Red bars: 48 hour biofilms. Asterisks indicate p-values < 0.01 using 2-tailed Student t-test (unpaired with unequal variance).

Interestingly, we did not observe improved tolerance to common osmotic agents, including glucose and sorbitol, in isolated adaptive mutants with mutations in *CgSTE11*. In *S. cerevisiae*, the acetate activated Hog1 was found to not enhance hyperosmotic tolerance⁴², suggesting complex regulation of the activity of Hog1. Therefore, it may be that the *CgSte11* variants did not lead to activation of Hog1, or activated Hog1 in a manner that did not impact the osmotolerance of *C. glabrata*. The exact mechanism remains to be investigated.

In response to various environmental stressors, cross-talk between different signaling cascades is necessary to coordinate the regulation of gene expression for cellular survival, especially when the stress level exceeds the capacity that can be mitigated by a single signaling cascade^{43,44}. Much of our knowledge on fungal signaling cascades come from studies in *S. cerevisiae*. The cell wall integrity (CWI) pathway orchestrates cellular responses such as cell wall biosynthesis and actin organization necessary for the cell to withstand various stresses⁴⁵. In *S. cerevisiae*, the CWI pathway is activated by heat stress⁵, involved in tolerance to low pH⁴⁶, and increased activation of the CWI pathway has been shown to enhance tolerance to isobutanol⁴⁷. Evidence have started to emerge showing that Ste11 plays a critical role in the cross-talk between the CWI and the HOG pathway in *S. cerevisiae* in response to environmental stressors, such as oxidative and thermal stress^{13,48}. Leng and Song reported that Nst1p mediates the interaction between Ste11p and Mkk1/2p, connecting the HOG and pheromone signaling pathways to the CWI pathway in response to heat and pheromone¹³. In addition, Jin *et al.* showed that in *S. cerevisiae*, Ste11p may activate Mkk1/2p and subsequently Slt2p and Kdx1p, which results in the nuclear release and subsequent degradation of the repressor cyclin C in response to high levels of oxidative stress to activate stress-responsive gene expression⁴⁸. Consistent with these reports, our data showed that mutations in *CgSTE11* conferred improved tolerance to both oxidative and thermal stress. Although differences exist, most of the components from the HOG and CWI pathway are conserved (at the sequence level) between *S. cerevisiae* and *C. glabrata*¹⁸. Given the high level of stressors used in this work, cross-talk between multiple signaling cascades, such as HOG and CWI pathways, may be involved in the ability of the isolated adaptive mutants to survive in these environmental stressors. Blast analysis of putative signaling proteins in the HOG and CWI pathways in *C. glabrata* (e.g. Ste11p [64% identity, 77% similarity], Mkk1p [58% identity, 67% similarity], Mkk2p [68% identity, 81% similarity], Nst1p [77% identity, 90% similarity], Slt2p [77% identity, 84% similarity]) showed that they have relatively high similarity and identity at the amino acid level to their putative *S. cerevisiae* orthologs. Further detailed studies are needed, however, to determine the extent of conservation between the MAPK signaling pathways between these two species.

In addition to the MAPK signaling pathways, heat shock proteins (HSP), which are involved in protein folding, prevention of protein aggregation, degradation and repair of damaged proteins, also play a crucial role for cell survival in environmental stressors. HSP90 family of HSPs is well-conserved among eukaryotic cells⁴⁹. In *S. cerevisiae*, the HSP90 family has two isomers, encoded by *HSP82* and *HSC82*⁵⁰. Although to different extents, the expression of both isomers of HSP90 are significantly induced in response to heat challenge in *S. cerevisiae*⁵⁰. Acting as an evolutionary capacitor, HSP90 is able to mask phenotypic effects of pre-existing genetic variants that are not adaptive to keep them from being lost in the evolving populations and to release their phenotypic effects rapidly when its activity is compromised (e.g. by environmental stress)^{51–54}, which facilitates evolutionary changes over long timescale. In addition, HSP90 has been proposed to function as a biological transistor that tunes cellular outputs (e.g. morphology, cell cycle progression, and drug resistance) to environmental inputs by regulating activities of core signaling pathways (e.g. CWI and Ca²⁺-calmodulin pathways)⁴⁹. Members of the MAPK signaling pathways, such as Ste11p and Slt2p, are among the numerous proteins that interact with members of the HSP90 family^{55,56}. Hsp90 is reported to impact the kinase activity of Ste11p in *S. cerevisiae*^{55,57}. In addition, it has also been reported that appropriate post-translational modifications of HSP90 is necessary for efficient chaperoning of Ste11p and Slt2p⁵⁸, suggesting that the chaperoning by HSP90 is important for Ste11p to function properly in signal transduction to regulate cellular response to environmental stressors. Indeed, our data showed that parental strains and isolated adaptive mutants with mutations in *CgSTE11* are hypersensitive to high temperature exposure

(41 °C) in the presence of the HSP90 inhibitor radicicol. Taken together, the results suggest that the activity of the CgSte11 depends on the chaperoning of the HSP90 in *C. glabrata* in a similar fashion to *S. cerevisiae*.

In addition to mutations in *CgSTE11*, several other mutations were identified in the isolated adaptive mutants. Interestingly, in population T2, temporal isolates exhibited increased tolerance to some stressors (e.g. HCl, ethanol, H₂O₂) as a function of time. As mutations in *CgSTE11* are already present in the earliest isolate (T2-5G), it strongly suggests that additional mutations found in the later isolates within the T2 population further contribute to environmental stress tolerance of *C. glabrata* to various abiotic stresses.

Conclusion

In this work, we identified significant cross-tolerance between heat and other environmental stressors such as oxidative, low pH, organic acid, and organic solvent in *C. glabrata* mutants evolved under periodic hyperthermal challenge. Focusing on the genotype-phenotype relationship in isolated adaptive clones, we demonstrated that mutations in *CgSTE11* is causative for the observed enhanced tolerance to heat and several other environmental stressors. Based on these results, we postulate that the identified mutations in *CgSTE11* likely led to enhanced activity of CgSte11, with impacts in multiple MAPK signal transduction cascades to enhance cellular resistance to several environmental stressors. Further experiments, especially detailed functional analysis of the mutated CgSte11 and components of the signaling pathways are needed to determine the exact molecular mechanism of how CgSte11 mediates tolerance to environmental stressors in *C. glabrata*. The work reported here shed light on the importance of the MAPK kinase kinase *STE11* in adaptation to environmental stressors in this important and yet under-studied organism.

Materials and Methods

Fungal strains and culture medium. Unless specified, Yeast Nitrogen Base (YNB) supplemented with 2% (w/v) dextrose is used as the media in all experiments. *C. glabrata* strains used in this study are derivatives of ATCC 2001. The primers, plasmids, and strains used in this study are listed in Supplementary Table S1.

The fluorescent *C. glabrata* strains, MHCg-Y and MHCg-G (as KKY and KKG, respectively, previously used in³⁴), were constructed as follows: the gene encoding green fluorescent protein (GFP) was amplified from pGS62 plasmid²² using primer pair of HE1_F and HE1_R; the gene encoding yellow fluorescent protein (YFP) was amplified from pGS63²² using primer pair HE2_F and HE2_R. The PCR products and the vector yEPGAP-cherry⁵⁹ were digested with EcoRI and XhoI. Each insert (GFP or YFP) was ligated with the vector backbone (replacing the yEMRFP gene on yEPGAP-cherry) to generate plasmids yEPGAP-GFP and yEPGAP-YFP, respectively. The SAT1 marker, amplified from yEP352-SAT1⁶⁰ plasmid using the primers HE4_F and HE4_R, was assembled with the SalI-digested yEPGAP-GFP and yEPGAP-YFP via Gibson assembly⁶¹ to create plasmid yEPGAP-GFP-SAT1 and yEPGAP-YFP-SAT1, respectively. Gibson assembly reactions were carried out using Phusion[®] High-Fidelity DNA Polymerase (NEB), Taq DNA ligase (NEB), and T5 exonuclease (NEB); and the reaction was incubated at 50 °C for 1 hour. The 5' and 3' flanking regions for the fluorescent integration cassettes were amplified from genomic DNA (gDNA) of ATCC 2001 using the primer pairs HE6_F and HE6_R and HE7_F and HE7_R respectively, which contain homologous sequences to the pseudo gene CAGL0C01067g. The GFP and YFP cassettes were amplified from yEPGAP-GFP-SAT1 and yEPGAP-YFP-SAT1, respectively; and then assembled with the two flanking regions and BamHI-digested plasmid yEPGAP-cherry by Gibson assembly to create the fluorescent integration plasmids yMH-Cgl-GFP and yMH-Cgl-YFP. The fluorescent integration plasmids were then digested with SphI and integrated into the genome of ATCC 2001 by electroporation⁶² to generate the fluorescently marked strains MHCg-G and MHCg-Y, respectively.

The mutant alleles of CAGL0B02739g (*CgSTE11*) identified from the three evolved populations (T1, T2, and T3) were introduced into ATCC 2001 by first amplifying the partial coding sequences (~985 bp) containing the desired mutations in CAGL0B02739g from the gDNA of T1-27G, T2-5G, or T3-24Y with primer pair TE9_F and TE9_R to generate the 1st part of the DNA fragment. The 2nd part (~367 bp) was synthesized as a gBlock DNA fragments (Integrated DNA Technologies, Inc) to remove the existing BsaI site via a single nucleotide substitution without causing an amino acid change; and was joined with the 1st part by overlapping PCR using the primer pair TE9_F and TE10_R. The partial coding sequence of the wild-type version of CAGL0B02739g was constructed in a similar way using the gDNA of ATCC 2001 as the template with the same primer pairs. The 3' untranslated region (3'UTR) of CAGL0B02739g was amplified from the gDNA of ATCC 2001 with primers TE11_F and TE11_R. In addition, the SAT1-FLP cassette was amplified from the plasmid yEP352-SAT1 with primers TE12_F and TE12_R. These DNA fragments were each first cloned into the entry vector pYTK001 from the Yeast Tool Kit³³ to create a set of part plasmids (pMH032, pMH033, pMH034, and pMH041, pMH042, and pMH043); and then were assembled with parts from pYTK002, pYTK067, and pYTK095 to construct four cassette plasmids pMH035, pMH036, pMH037, and pMH038 that contain the replacement cassettes for mutant alleles of CAGL0B02739g from populations T1, T2, T3 and the wild-type control, respectively. These plasmid constructions follow the MoClo-derived assembly described by Lee, *et al.*³³. The part plasmids used in the construction of the replacement cassette plasmids were verified by Sanger sequencing. Each replacement cassette was digested from the cassette plasmids by BsmBI (Thermo scientific) and integrated into the genome of ATCC 2001 using the Easy Frozen-EZ Yeast Transformation II Kit (Zymo Research) following the manufacturer recommended protocol. Positive transformants were selected on nourseothricin (100 µg/mL) YPD plates. The SAT1-FLP cassette was looped out spontaneously by growing the transformants in YPD medium without nourseothricin and subsequently verified by both colony PCR using primers TE25_F and TE25_R and Sanger sequencing.

The *C. glabrata ste11Δ* deletion strain (*ste11::SAT1 his3Δ leu2Δ trp1Δ*) was a gift from Karl Kuchler at the Medical University Vienna. All strains used in experiments comparing the *ste11Δ* strain were cultured in synthetic complete (SC) media.

Adaptive evolution of *C. glabrata* to thermal stress. The adaptive laboratory evolution experiments were carried out in 25 ml cultures in 125 ml flasks at 30 °C. The starting populations consisted of approximately equal numbers of MHCg-G and MHCg-Y strains. Three populations (T1, T2, and T3) were evolved in parallel. Each population was serially transferred daily and periodically heat-challenged following a two-phase strategy (Fig. 1a). During Phase I (P1), 1 ml of cell culture after 24-hour growth was challenged with heat stress for 30 minutes, followed by inoculation into 24 ml of fresh growth medium for overnight recovery and growth. In Phase 2 (P2), 250 µl of the overnight culture from the P1 phase was transferred into 24.75 ml of fresh growth medium; and the cells were grown for 24 hours to allow further recovery from the heat challenge. The two-phase strategy was repeated until the end of the evolution. During the evolution, the OD₆₀₀ of the populations were measured by sampling the culture before and after each transfer. Frozen stocks of the evolving populations sampled immediately before each stress challenge were prepared in 25% (v/v) glycerol and stored at -80 °C for future characterizations. When a significant increase in OD₆₀₀ is observed after the second recovery phase, the thermotolerance of the evolving populations was measured using a modified method used for the general stress tolerance (described in the “Phenotypic characterizations of adaptive clones and population samples” section below) to confirm any improvements in hyperthermal tolerance. Briefly, the population samples were challenged with a temperature gradient starting from the current level used during evolution to 2 °C above (in 1 °C increment) for 30 minutes; the remaining steps were unchanged. The selective pressure (temperature) was ramped up to the new level that led to at least a 10-fold reduction in viability compared to the control (challenged at 30 °C). The relative proportions of the two subpopulations (MHCg-G and MHCg-Y) within each evolving population was measured using FACSscan flow cytometer (BD Biosciences, San Jose, CA). The isolation of the adaptive mutant for a given population sample was performed as follows: a minimum of 8 colonies from a given population sample were randomly chosen and their relative thermotolerance were estimated using the general stress tolerance protocol described above; the isolate with the highest heat tolerance was selected as the adaptive mutant from that population. The naming of the adaptive mutants is based on the population samples from which they were isolated and the color of the fluorescent protein expressed (e.g. mutant T2-5G was isolated from the GFP subpopulation from time point 5 of population T2).

Phenotypic characterizations of adaptive clones and population samples. *Survival assay.* The thermo-tolerance of population samples and isolated mutants were assessed after one-hour exposure to the temperature at which the samples were challenged at during the evolution experiment. Each sample was grown to an OD₆₀₀ between 2.0–3.0 in YNB supplemented with 2% (w/v) dextrose at 30 °C, then the OD₆₀₀ was normalized to ~0.5 before the heat challenge. 500 µl of the normalized samples were challenged with heat stress for 1 hour with shaking at 250 RPM in a shaking incubator; cells in the control group were incubated at 30 °C for 1 hour in a shaker. After the challenge, the cells (both control and heat-challenged groups) were placed on ice for 5 minutes, then subjected to serial 10-fold dilutions using culture medium; and the 10⁻⁴-fold diluted cells were plated on YNB plates and incubated at 30 °C for two days before counting the number of colony forming units (CFUs). The survival rate was calculated as the ratio of the CFUs of heat-challenged cells to CFUs of the control group. At least three biological replicates for each sample were used.

General stress tolerance. The stress tolerance of isolated adaptive mutants was characterized using the following steps: 1) cultures were grown to an OD₆₀₀ between 2.0–3.0 in YNB at 30 °C, 2) the OD₆₀₀ was normalized to ~0.5 for heat and ~1.0 for other stresses before the challenge, and 3) 500 µl of the normalized samples were then challenged by the stressor-of-interest for 1 hour in a shaker. For the control group, cells were incubated in the absence of stressor for 1 hour at 30 °C in a shaker. The stressors used include 4% (v/v) isobutanol, 4% (v/v) 1-butanol, 16% (v/v) ethanol, 0.2 M of HCl (pH~1.0), 0.2 M of acetic acid (pH~3.0), 100 mM of H₂O₂, and heat at 47 °C and 50 °C. For the stressors other than heat, the cells (both control and stress-challenged group) were pelleted after the challenge to remove the supernatant and then serially diluted (10-fold dilutions) using culture medium. For heat stress, the cells (both control and heat-shocked groups) were placed on ice for 5 minutes after the challenge before subjected to serial 10-fold dilutions using YNB. 5 µl of diluted cells (10⁻¹, 10⁻², 10⁻³, and 10⁻⁴) were spotted on YNB agar medium supplemented with 2% dextrose and incubated at 30 °C for two days and photographed for analysis.

We also evaluated the tolerance of adaptive mutants to osmotic stressors (glucose and sorbitol) and antibiotics (amphotericin B and fluconazole) in YNB medium. For osmotic stressors, we cultured 200 µl of cells with OD₆₀₀ normalized to ~0.02 in YNB medium in the presence of a concentration gradient of glucose (0%, and 20% to 35% w/v with 5% increment) and sorbitol (0 M, and 1.5 M to 3 M with 0.5 M increment) in 96-well plates at 30 °C and 200 rpm. The OD₆₀₀ was measured using a microplate reader (Tecan Group Ltd., Switzerland). Growth curve fitting of OD₆₀₀ data with the late-stationary-phase time points excluded was performed using DMFit (www.ifr.ac.uk/safety/DMfit) to measure specific growth rates using the model of Baranyi and Roberts⁶³. For antibiotics, a modified test based on the CLSI broth microdilution method⁶⁴ was performed via the following steps: (1) cells were grown on SDA plates (1% Peptone, 4% Dextrose, 1.5% agar, adjusted to pH 5.6 with HCl) at 35 °C for 24 hours, (2) 4 or 5 colonies ~1 mm in diameter were picked from the SDA plates and suspended in 1 ml of sterile 0.85% saline (8.5 g/L NaCl in water), (3) the OD₆₀₀ was normalized to ~0.5 and the normalized cultures were diluted 50 fold first using 0.85% saline, followed by 50-fold and 5-fold dilution using YNB medium, (4) 100 µl of the diluted cultures were then mixed with 100 µl of YNB medium containing a concentration gradient of amphotericin B (0, and 0.25 µg/mL to 32 µg/mL in 2-fold serial dilution) or fluconazole (0, 1 µg/mL to 128 µg/mL in 2-fold serial dilution) in 96-well plate, (5) the 96-well plate were incubated at 35 °C without agitation for 48 hours in the dark, and (6) the OD₄₉₂ of cell contents in each well of the 96-well plate was measured to estimate the biomass. The minimal inhibitory concentration (MIC) of antibiotics which result in at least 50% reduction in the biomass as compared to control (0 µg/mL) was determined using two biological replicates.

Radical treatment. Radicol functions as an inhibitor of Hsp90⁶⁵ and was used to assess whether the hyperthermal tolerance in the isolated mutants is Hsp90-dependent. Radicol (Cayman chemical) was dissolved in DMSO to make the stock solution (2 mg/ml). The impact of radicol on the hyperthermal tolerance of each strain was determined by normalizing overnight cultures of each strain (OD₆₀₀ between 2.0–3.0) grown in YNB at 30 °C to an OD₆₀₀ of ~0.5. The normalized samples were serially diluted in YNB, and 5 µl of diluted cells (10⁻¹, 10⁻², 10⁻³, and 10⁻⁴) were spotted on YNB agar medium supplemented with 2% (w/v) dextrose and 5 µM of radicol. A control group spotted on YNB agar or YNB agar with or without 0.09% (v/v) DMSO in the absence of radicol were included. Each set of samples were incubated at 30 °C and 41 °C for two days and photographed for analysis.

Biofilm quantification assay. Single colonies of *C. glabrata* strains (ATCC 2001, sMH080, sMH081, sMH082, ste11Δ) were picked from agar plates and cultured in YPD broth at 37 °C. Overnight cultures were washed twice with PBS and resuspended in fresh YPD medium to a concentration of 2.5 × 10⁷/ml using a hemocytometer. 100 µl of cell suspension was added to each well of 96-well plates precoated with type I collagen (Corning BioCoat, Fisher Scientific). The cells were cultured for 24 h or 48 h at 37 °C without agitation for biofilm formation. Unattached cells and media were removed by inverting the plates, and tapping the plates gently on paper towels twice. Following a similar procedure, the established biofilms were washed twice with 200 µl PBS, then air dried. Once completely dried, 200 µl of 0.1% crystal violet was added to each well and incubated at room temperature for 20 minutes⁶⁶. The plates were then submerged in a tray of DI water, inverted to remove water, and tapped two times to remove excess crystal violet stain from the wells and biofilms. 150 µl of 33% acetic acid was added to each well, and absorbance was measured at 590 nm in a plate reader (Neo2S Biotek). Three biological replicates with three technical replicates each were used for analysis.

Next-Gen sequencing. The adaptive clones, T1-27G, T2-5G, T2-10G, T2-17G, T2-27G, and T3-24Y, from population T1, T2, and T3 and the two unevolved parental strains, MHCg-Y and MHCg-G were sequenced to identify the genetic mutations underlying the observed hyperthermal tolerance. In addition, temporal population samples from T1, T2, and T3 were sequenced as well in order to discover rare adaptive mutations (≥10%) and evaluate the temporal change in the population frequency of mutations. Genomic DNA was extracted using the YeaStar™ Genomic DNA kit (Zymo Research). Genomic library preparation and sequencing were performed by the Texas A&M Genomics Center for sequencing on the Illumina HiSeq 2500 platform using 100-bp pair-end reads. An average coverage of more than 32-fold was obtained for each clone, and ~200-fold for population samples. The raw sequencing data of these samples were deposited in SRA database (<https://www.ncbi.nlm.nih.gov/sra>) with accession number SRP112804. Reads were assembled against the CBS138 (ATCC 2001) reference genome, and each mutant genome was compared to the parental sequences to identify any *de novo* mutations using the CLC Genomics workbench (version 6.0.1). For calling of variants, the frequency threshold was set to be 90% for clones and 10% for population samples, and the forward/reverse balance was set at ≥0.3 for both. Otherwise, the default setting was used for the CLC Genomics workbench. Selected mutations were verified with Sanger sequencing and analyzed with Unipro UGENE.

Bioinformatics analysis. The Gene Ontology (GO) analysis tool from Candida Genome Database (CGD)⁶⁷ was used to identify any enriched biological processes and functional categories in the mutated genes. Since a large fraction (95.67%) of the genes in *C. glabrata* have not been characterized in detail⁶⁷, functions of genes-of-interest were inferred based on their *S. cerevisiae* orthologs using available information from the Saccharomyces Genome Database (SGD)⁶⁸.

Data availability

The datasets of genome sequencing generated during the current study are available in the SRA database with accession number SRP112804, <https://www.ncbi.nlm.nih.gov/sra>. All other data generated or analyzed during this study are included in this published article (and its Supplementary Information Files).

Received: 28 November 2017; Accepted: 29 October 2019;

Published online: 19 November 2019

References

1. Attfield, P. V. Stress tolerance: The key to effective strains of industrial baker's yeast. *Nat Biotechnol* **15**, 1351–1357 (1997).
2. Lindquist, S. Heat-shock proteins and stress tolerance in microorganisms. *Current Opinion in Genetics & Development* **2**, 748–755 (1992).
3. Rodríguez-Peña, J. M., García, R., Nombela, C. & Arroyo, J. The high-osmolarity glycerol (HOG) and cell wall integrity (CWI) signalling pathways interplay: a yeast dialogue between MAPK routes. *Yeast* **27**, 495–502 (2010).
4. Mensonides, F., Brul, S., Klis, F. M., Hellingwerf, K. J. & de Mattos, M. Activation of the protein kinase C1 pathway upon continuous heat stress in *Saccharomyces cerevisiae* is triggered by an intracellular increase in osmolarity due to trehalose accumulation. *Appl Environ Microbiol* **71**, 4531–4538 (2005).
5. Kamada, Y., Jung, U. S., Piotrowski, R. & Levin, D. E. The Protein-Kinase C-Activated Map Kinase Pathway of *Saccharomyces cerevisiae* Mediates a Novel Aspect of the Heat-Shock Response. *Genes and Development* **9**, 1559–1571 (1995).
6. Winkler, A. *et al.* Heat stress activates the yeast high-osmolarity glycerol mitogen-activated protein kinase pathway, and protein tyrosine phosphatases are essential under heat stress. *Eukaryotic Cell* **1**, 163–173 (2002).
7. Tanaka, K. *et al.* Yeast Osmosensors Hkr1 and Msb2 Activate the Hog1 MAPK Cascade by Different Mechanisms. *Science Signaling* **7**, ra21–ra21 (2014).
8. Tatebayashi, K. *et al.* Osmosensing and scaffolding functions of the oligomeric four-transmembrane domain osmosensor Sho1. *Nature Communications* **6** (2015).
9. Posas, F. *et al.* Yeast HOG1 MAP kinase cascade is regulated by a multistep phosphorelay mechanism in the SLN1-YPD1-SSK1 “two-component” osmosensor. *Cell* **86**, 865–875 (1996).
10. Gray, J. V. *et al.* A role for the Pkc1 MAP kinase pathway of *Saccharomyces cerevisiae* in bud emergence and identification of a putative upstream regulator. *Embo* **16**, 4924–4937 (1997).

11. Ketela, T., Green, R. & Bussey, H. Saccharomyces cerevisiae Mid2p is a potential cell wall stress sensor and upstream activator of the PKC1-MPK1 cell integrity pathway. *J Bacteriol* **181**, 3330–3340 (1999).
12. Lee, K. S. *et al.* A Yeast Mitogen-Activated Protein-Kinase Homolog (Mpk1p) Mediates Signaling by Protein-Kinase-C. *Mol Cell Biol* **13**, 3067–3075 (1993).
13. Leng, G. & Song, K. Direct interaction of Ste11 and Mkk1/2 through Nst1 integrates high-osmolarity glycerol and pheromone pathways to the cell wall integrity MAPK pathway. *FEBS Lett* **590**, 148–160 (2015).
14. Yamamoto, N., Maeda, Y., Ikeda, A. & Sakurai, H. Regulation of thermotolerance by stress-induced transcription factors in *Saccharomyces cerevisiae*. *Eukaryotic Cell* **7**, 783–790 (2008).
15. Zähringer, H., Thevelein, J. M. & Nwaka, S. Induction of neutral trehalase Nth1 by heat and osmotic stress is controlled by STRE elements and Msn2/Msn4 transcription factors: variations of PKA effect during stress and growth. *Mol Microbiol* **35**, 397–406 (2000).
16. Gasch, A. P. *et al.* Genomic expression programs in the response of yeast cells to environmental changes. *Mol Biol Cell* **11**, 4241–4257 (2000).
17. Leach, M. D. & Cowen, L. E. To sense or die: mechanisms of temperature sensing in fungal pathogens. *Curr Fungal Infect Rep* **8**, 185–191 (2014).
18. Nikolaou, E. *et al.* Phylogenetic diversity of stress signalling pathways in fungi. *BMC Evolutionary Biology* **9**, 44 (2009).
19. Roetzer, A., Gabaldón, T. & Schüller, C. From *Saccharomyces cerevisiae* to *Candida glabrata* in a few easy steps: important adaptations for an opportunistic pathogen. *FEMS Microbiol Lett* **314**, 1–9 (2011).
20. Roetzer, A. *et al.* *Candida glabrata* environmental stress response involves *Saccharomyces cerevisiae* Msn2/4 orthologous transcription factors. *Mol Microbiol* **69**, 603–620 (2008).
21. Gregori, C. *et al.* The high-osmolarity glycerol response pathway in the human fungal pathogen *Candida glabrata* strain ATCC 2001 lacks a signaling branch that operates in baker's yeast. *Eukaryotic Cell* **6**, 1635–1645 (2007).
22. Kao, K. C. & Sherlock, G. Molecular characterization of clonal interference during adaptive evolution in asexual populations of *Saccharomyces cerevisiae*. *Nat Genet* **40**, 1499–1504 (2008).
23. Leyer, G. J. & Johnson, E. A. Acid Adaptation Induces Cross-Protection Against Environmental Stresses in *Salmonella Typhimurium*. *Appl Environ Microbiol* **59**, 1842–1847 (1993).
24. Dragosits, M., Mozhaykiy, V., Quinones-Soto, S., Park, J. & Tagkopoulos, I. Evolutionary potential, cross-stress behavior and the genetic basis of acquired stress resistance in *Escherichia coli*. *Mol Syst Biol* **9**, 1–13 (2013).
25. Oide, S. *et al.* Thermal and solvent stress cross-tolerance conferred to *Corynebacterium glutamicum* by adaptive laboratory evolution. *Appl Environ Microbiol* **81**, 2284–2298 (2015).
26. Calcagno, A.-M. *et al.* *Candida glabrata* Ste11 is involved in adaptation to hypertonic stress, maintenance of wild-type levels of filamentation and plays a role in virulence. *Medical Mycology* **43**, 355–364 (2005).
27. Jarolim, S. *et al.* *Saccharomyces cerevisiae* genes involved in survival of heat shock. *G3 (Bethesda)* **3**, 2321–2333 (2013).
28. Ding, J. *et al.* Acetic acid inhibits nutrient uptake in *Saccharomyces cerevisiae*: auxotrophy confounds the use of yeast deletion libraries for strain improvement. *Appl Microbiol Biotechnol* **97**, 7405–7416 (2013).
29. Brown, J. A. *et al.* Global analysis of gene function in yeast by quantitative phenotypic profiling. *Mol Syst Biol* **2** (2006).
30. Teixeira, M. C., Raposo, L. R., Mira, N. P., Lourenco, A. B. & Sá-Correia, I. Genome-Wide Identification of *Saccharomyces cerevisiae* Genes Required for Maximal Tolerance to Ethanol. *Appl Environ Microbiol* **75**, 5761–5772 (2009).
31. Schmidt, M., Akasaka, K., Messerly, J. T. & Boyer, M. P. Role of Hog1, Tps1 and Sod1 in boric acid tolerance of *Saccharomyces cerevisiae*. *Microbiology (Reading, Engl)* **158**, 2667–2678 (2012).
32. Ho, H.-L. & Haynes, K. *Candida glabrata*: new tools and technologies—expanding the toolkit. *FEMS Yeast Research* **15**, fov066 (2015).
33. Lee, M. E., DeLoache, W. C., Cervantes, B. & Dueber, J. E. A Highly Characterized Yeast Toolkit for Modular, Multipart Assembly. *ACS Synth. Biol.* **4**, 975–986 (2015).
34. Huang, M. & Kao, K. C. Identifying novel genetic determinants for oxidative stress tolerance in *Candida glabrata* adaptive laboratory evolution. *Yeast*, <https://doi.org/10.1002/yea.3352> (2018).
35. Curran, K. A. *et al.* Short Synthetic Terminators for Improved Heterologous Gene Expression in Yeast. *ACS Synth. Biol.* **4**, 824–832 (2015).
36. Reynolds, T. B. & Fink, G. R. Bakers' Yeast, a Model for Fungal Biofilm Formation. *Science* **291**, 878–881 (2001).
37. Fanning, S. *et al.* Functional control of the *Candida albicans* cell wall by catalytic protein kinase A subunit Tpk1. *Mol Microbiol* **86**, 284–302 (2012).
38. Li, Z. *et al.* Involvement of glycolysis/gluconeogenesis and signaling regulatory pathways in *Saccharomyces cerevisiae* biofilms during fermentation. *Front. Microbio.* **6** (2015).
39. Konstantinidou, N. & Morrissey, J. P. Co-occurrence of filamentation defects and impaired biofilms in *Candida albicans* protein kinase mutants. *FEMS Yeast Research* **15**, fov092 (2015).
40. Singh, K. K. The *Saccharomyces cerevisiae* sln1p-ssk1p two-component system mediates response to oxidative stress and in an oxidant-specific fashion. *Free Radic. Biol. Med.* **29**, 1043–1050 (2000).
41. Bilsland, E., Molin, C., Swaminathan, S., Ramne, A. & Sunnerhagen, P. Rck1 and Rck2 MAPKAP kinases and the HOG pathway are required for oxidative stress resistance. *Mol Microbiol* **53**, 1743–1756 (2004).
42. Mollapour, M. & Piper, P. W. Hog1p mitogen-activated protein kinase determines acetic acid resistance in *Saccharomyces cerevisiae*. *FEMS Yeast Research* **6**, 1274–1280 (2006).
43. Junttila, M. R., Li, S.-P. & Westermarck, J. Phosphatase-mediated crosstalk between MAPK signalling pathways in the regulation of cell survival. *FASEB J.* **22**, 954–965 (2008).
44. Saito, H. Regulation of cross-talk in yeast MAPK signaling pathways. *Current Opinion in Microbiology* **13**, 677–683 (2010).
45. Levin, D. E. Cell wall integrity signaling in *Saccharomyces cerevisiae*. *Microbiology and Molecular Biology Reviews* **69**, 262–+ (2005).
46. Lucena, R. M., Elsztein, C., Simões, D. A. & Morais, M. A. Participation of CWI, HOG and Calcineurin pathways in the tolerance of *Saccharomyces cerevisiae* to low pH by inorganic acid. *J Appl Microbiol* **113**, 629–640 (2012).
47. Bramucci, M. G., Larossa, R. A. & Smulski, D. R Butamax Advanced Biofuels LLC. Yeast with increased butanol tolerance involving cell wall integrity pathway (2010).
48. Jin, C., Kim, S. K., Willis, S. D. & Cooper, K. F. The MAPKKs Ste11 and Bck1 jointly transduce the high oxidative stress signal through the cell wall integrity MAP kinase pathway. *Microb Cell* **2**, 329–342 (2015).
49. Leach, M. D., Klipp, E., Cowen, L. E. & Brown, A. J. P. Fungal Hsp90: a biological transistor that tunes cellular outputs to thermal inputs. *Nat Rev Microbiol* **10**, 693–704 (2012).
50. Borkovich, K. A., Farrelly, F. W., Finkelstein, D. B., Taulien, J. & Linquist, S. Hsp82 Is an Essential Protein That Is Required in Higher Concentrations for Growth of Cells at Higher Temperatures. *Mol Cell Biol* **9**, 3919–3930 (1989).
51. Cowen, L. E. & Lindquist, S. Hsp90 potentiates the rapid evolution of new traits: drug resistance in diverse fungi. *Science* **309**, 2185–2189 (2005).
52. Jaros, D. F. & Lindquist, S. Hsp90 and Environmental Stress Transform the Adaptive Value of Natural Genetic Variation. *Science* **330**, 1820–1824 (2010).
53. Rutherford, S. L. & Linquist, S. Hsp90 as a capacitor for morphological evolution. *Nature* **396**, 336–342 (1998).

54. Chen, G., Bradford, W. D., Seidel, C. W. & Li, R. Hsp90 stress potentiates rapid cellular adaptation through induction of aneuploidy. *Nature* **482**, 246–250 (2012).
55. Louvion, J.-F., Abbas-Terki, T. & Picard, D. Hsp90 Is Required for Pheromone Signaling in Yeast. *Mol Biol Cell* **9**, 3071–3083 (1998).
56. Millson, S. H. *et al.* Investigating the protein-protein interactions of the yeast Hsp90 chaperone system by two-hybrid analysis: potential uses and limitations of this approach. *Cell Stress Chaperones* **9**, 359–368 (2004).
57. Mishra, P., Flynn, J. M., Starr, T. N. & Bolon, D. N. A. Systematic Mutant Analyses Elucidate General and Client-Specific Aspects of Hsp90 Function. *CellReports* **15**, 588–598 (2016).
58. Mollapour, M. *et al.* Swe1Wee1-dependent tyrosine phosphorylation of Hsp90 regulates distinct facets of chaperone function. *Molecular Cell* **37**, 333–343 (2010).
59. Keppler-Ross, S., Noffz, C. & Dean, N. A New Purple Fluorescent Color Marker for Genetic Studies in *Saccharomyces cerevisiae* and *Candida albicans*. **179**, 705–710 (2008).
60. Krauke, Y. & Sychrova, H. Cnh1 Na(+)/H(+) antiporter and Ena1 Na(+)-ATPase play different roles in cation homeostasis and cell physiology of *Candida glabrata*. *FEMS Yeast Research*, <https://doi.org/10.1111/j.1567-1364.2010.00686.x> (2010).
61. Gibson, D. G. *et al.* Enzymatic assembly of DNA molecules up to several hundred kilobases. *Nat Meth* **6**, 343–345 (2009).
62. Reuss, O., Vik, A., Kolter, R. & Morschhäuser, J. The SAT1 flipper, an optimized tool for gene disruption in *Candida albicans*. *Gene* **341**, 119–127 (2004).
63. Baranyi, J. & Roberts, T. A. A Dynamic Approach to Predicting Bacterial-Growth in Food. *Int J Food Microbiol* **23**, 277–294 (1994).
64. NCCLS. M27-A2 Reference Method for Broth Dilution Antifungal Susceptibility Testing of Yeasts; Approved Standard—Second Edition. 1–51 (2002).
65. Roe, S. M. *et al.* Structural basis for inhibition of the Hsp90 molecular chaperone by the antitumor antibiotics radicicol and geldanamycin. *J. Med. Chem.* **42**, 260–266 (1999).
66. Peeters, E., Nelis, H. J. & Coenye, T. Comparison of multiple methods for quantification of microbial biofilms grown in microtiter plates. *J. Microbiol. Methods* **72**, 157–165 (2008).
67. Skrzypek, M. S. *et al.* The *Candida* Genome Database (CGD): incorporation of Assembly 22, systematic identifiers and visualization of high throughput sequencing data. *Nucleic Acids Research* **45**, D592–D596 (2017).
68. Cherry, J. M. *et al.* *Saccharomyces* Genome Database: the genomics resource of budding yeast. *Nucleic Acids Research* **40**, D700–D705 (2011).

Acknowledgements

We thank Xinhe Chen for her assistance in the construction of the *CgSTE11* variants and NSF (MCB-1054276 to K.C.K.), NIH (R15AI138146 to A.K.R.) and Texas A&M Genomics Seed Grant for partial financial support of this project. The *ste11Δ* strain was a gift from Karl Kuchler at Medical University Vienna.

Author contributions

M.H. conception and design, collection and assembly of data, data analysis, and manuscript writing; J.K. collection and assembly of data; M.K. collection and assembly of data; J.D.T.V. collection and assembly of data; O.A.A.P. collection and assembly of data; A.K.R. data analysis and financial support; K.C.K. data analysis, manuscript writing, financial support, and final approval of the manuscript.

Competing interests

The authors declare no competing interests.

Additional information

Supplementary information is available for this paper at <https://doi.org/10.1038/s41598-019-53593-5>.

Correspondence and requests for materials should be addressed to K.C.K.

Reprints and permissions information is available at www.nature.com/reprints.

Publisher's note Springer Nature remains neutral with regard to jurisdictional claims in published maps and institutional affiliations.



Open Access This article is licensed under a Creative Commons Attribution 4.0 International License, which permits use, sharing, adaptation, distribution and reproduction in any medium or format, as long as you give appropriate credit to the original author(s) and the source, provide a link to the Creative Commons license, and indicate if changes were made. The images or other third party material in this article are included in the article's Creative Commons license, unless indicated otherwise in a credit line to the material. If material is not included in the article's Creative Commons license and your intended use is not permitted by statutory regulation or exceeds the permitted use, you will need to obtain permission directly from the copyright holder. To view a copy of this license, visit <http://creativecommons.org/licenses/by/4.0/>.

© The Author(s) 2019